Journal of Cerebral Blood Flow & Metabolism (2012) 32, 792–804

www.jcbfm.com

Insulin-induced generation of reactive oxygen species and uncoupling of nitric oxide synthase underlie the cerebrovascular insulin resistance in obese rats

Prasad VG Katakam[1,2], James A Snipes[2], Mesia M Steed[2] and David W Busija[1,2]

[1]*Department of Pharmacology, Tulane University School of Medicine, New Orleans, Louisiana, USA;* [2]*Department of Physiology and Pharmacology, Wake Forest University School of Medicine, Winston-Salem, North Carolina, USA*

Hyperinsulinemia accompanying insulin resistance (IR) is an independent risk factor for stroke. The objective is to examine the cerebrovascular actions of insulin in Zucker obese (ZO) rats with IR and Zucker lean (ZL) control rats. Diameter measurements of cerebral arteries showed diminished insulin-induced vasodilation in ZO compared with ZL. Endothelial denudation revealed vasoconstriction to insulin that was greater in ZO compared with ZL. Nonspecific inhibition of nitric oxide synthase (NOS) paradoxically improved vasodilation in ZO. Scavenging of reactive oxygen species (ROS), supplementation of tetrahydrobiopterin (BH_4) precursor, and inhibition of neuronal NOS or NADPH oxidase or cyclooxygenase (COX) improved insulin-induced vasodilation in ZO. Immunoblot experiments revealed that insulin-induced phosphorylation of Akt, endothelial NOS, and expression of GTP cyclohydrolase-I (GTP-CH) were diminished, but phosphorylation of PKC and ERK was enhanced in ZO arteries. Fluorescence studies showed increased ROS in ZO arteries in response to insulin that was sensitive to NOS inhibition and BH_4 supplementation. Thus, a vicious cycle of abnormal insulin-induced ROS generation instigating NOS uncoupling leading to further ROS production underlies the cerebrovascular IR in ZO rats. In addition, decreased bioavailability and impaired synthesis of BH_4 by GTP-CH induced by insulin promoted NOS uncoupling.
Journal of Cerebral Blood Flow & Metabolism (2012) **32,** 792–804; doi:10.1038/jcbfm.2011.181; published online 11 January 2012

Keywords: cerebral arteries; cyclooxygenase; GTP cyclohydrolase; superoxide; tetrahydrobiopterin; Zucker rats

Introduction

Type 2 diabetes (T2DM) affects over a fifth of people over the age of 65 years in the United States (Center for Disease Control and Prevention. National Diabetes Fact Sheet, 2011). Another 35% of people who are 65 years and older have prediabetes that usually begins as insulin resistance (IR), a disorder in which cells fail to use insulin properly, leading to increased insulin levels to maintain normal glucose levels. Individuals with IR and T2DM exhibit sustained hyperinsulinemia that has been implicated in cerebrovascular dysfunction (Erdos *et al*, 2004; Phillips *et al*, 2005) and enhanced stroke injury (Matsumoto *et al*, 1999).

Insulin, a metabolic hormone, has been known to exert vasodilator (Chen and Messina, 1996; Katakam *et al*, 2005; Oltman *et al*, 2000, 2006) as well as vasoconstrictor (Eringa *et al*, 2002; Katakam *et al*, 2009*a*; Miller *et al*, 2002; van Veen and Chang, 1998) effects on several diverse vascular beds. Recently, we identified insulin receptors in rat cerebral arteries and have reported the cerebrovascular actions of insulin (Katakam *et al*, 2009*b*). Cerebral arteries are subjected to hyperinsulinemia in IR and T2DM; however, the impact of insulin on cerebral vasoreactivity in IR has never been examined.

We hypothesized that cerebrovascular IR accompanies metabolic IR in Zucker obese (ZO) rats compared with Zucker lean (ZL) controls. In the present study, we identified the insulin receptors and determined the cerebrovascular actions of insulin in ZO and ZL rats. We also evaluated the endothelium- and vascular smooth muscle-dependent mechanisms involving cyclooxygenase (COX),

Correspondence: Dr PVG Katakam, 1430 Tulane Avenue, SL83, New Orleans, LA 70112, USA.
E-mail: pkatakam@tulane.edu
This study was supported by the National Institutes of Health Grants (HL-077731, HL-030260, HL093554, and HL-065380) awarded to Dr Busija.
Received 21 June 2011; revised 30 September 2011; accepted 3 November 2011; published online 11 January 2012

nitric oxide synthase (NOS), tetrahydrobiopterin (BH_4), GTP cyclohydrolase-I (GTP-CH), and reactive oxygen species (ROS) derived from NADPH oxidase. Finally, we determined the intracellular signaling pathways mediating the cerebrovascular actions of insulin in IR.

Materials and methods

The animal protocol was approved by the Institutional Animal Care and Use Committee of Wake Forest University Health Sciences and Tulane University. All experiments complied with the National Institute of Health (NIH) *Guide for the Care and Use of Laboratory Animals*. Young Sprague-Dawley (SD, $n = 10$), ZO ($n = 25$), and ZL ($n = 25$) rats were obtained at 10 to 11 weeks of age and aged SD rats ($n = 8$) were obtained at 12 months of age. Animals were housed in the animal care facility, received standard rat chow and tap water *ad libitum*.

Zucker Obese Rat Model

The ZO rat with a leptin receptor mutation (*fa/fa*, homozygous for the mutation) has been widely used as a model of IR and T2DM with ZL as genetically appropriate controls (*Fa/fa*, heterozygous for the mutation; Bray, 1977). Previous data from our laboratory (Erdos *et al*, 2004, 2006) and others (Oltman *et al*, 2006; Phillips *et al*, 2005; Stepp, 2006) have shown that ZO rats develop IR with a metabolic profile very similar to the human condition. As reported previously (Erdos *et al*, 2004, 2006), at 10 to 12 weeks of age, ZO rats had significantly greater body weight and exhibited features typical of metabolic syndrome including impaired glucose tolerance, hyperinsulinemia (widely used marker of IR), hypertriglyceridemia, and hypercholesterolemia. Importantly, young ZO rats used in the present study were insulin resistant but glucose levels and blood pressure were not elevated.

Insulin and Glucose Assays

Blood samples were taken via needle and syringe from the left ventricle after exposure to isofluorane anesthesia before decapitation of fasting rats. Plasma insulin and glucose levels were measured using a rat insulin enzyme-linked immunosorbent assay (ELISA) kit (Crystal Chem, Chicago, IL, USA) and Trinder reagent (Sigma, St Louis, MO, USA), respectively.

Vascular Reactivity

Arterial diameter studies were performed as described previously (Katakam *et al*, 2009*b*). Briefly, isolated middle and posterior cerebral arteries (140 to 180 μm) were cannulated in a vessel bath (Chueltech Scientific Design, Houston, TX, USA) filled with warm oxygenated (20%O_2/5% CO_2/75% N_2 at 37°C) physiological salt solution, and intraluminal diameter was measured by a video dimension analyzer (Living Systems, Burlington, VT, USA). Arteries were slowly pressurized to 70 mm Hg with physiological salt solution under no flow conditions until a stable myogenic tone (30% to 45% of passive diameter) developed. Subsequently, drugs were administered abluminally in the bath solution. Endothelium was removed by injecting a bolus of 1 mL of air through the arteries and confirmed by the lack of significant response to bradykinin. Each arterial segment was used only for a single dose–response experiment. Viability of all arteries was verified by contraction to 60 mmol/L potassium chloride (KCl), endothelium-dependent vasodilation to bradykinin- and vascular smooth muscle cell-dependent vasodilation to sodium nitroprusside. Previously, we reported that vascular parameters and responses of the middle and posterior cerebral arteries to insulin were similar to each other (Katakam *et al*, 2009*a*); therefore, the data were combined in the present study.

Vascular responses to insulin (0.1 to 100 ng/mL; Humulin R, Eli Lilly Company, Indianapolis, IN, USA) were determined in the presence and absence of indomethacin (nonselective COX inhibitor, 10 μmol/L), N^{ω}-nitro L-arginine methyl ester (L-NAME, nonselective NOS inhibitor, 100 μmol/L), 7-nitroindazole (7-NI, neuronal NOS (nNOS) inhibitor , 10 μmol/L), sepiapterin (a precursor of BH_4, 10 μmol/L), apocynin (NADPH oxidase inhibitor, 300 μmol/L), poly-ethylene glycol-superoxide dismutase (PEG-SOD, a membrane permeable ROS scavenger, 250 units/mL), and manganese(III) tetrakis(4-benzoic acid)porphyrin chloride (MnTBAP, a membrane permeable SOD mimetic, 100 μmol/L).

In-Situ Determination of Reactive Oxygen Species Generation

Dihydroethidium (DHE; Molecular Probes, Eugene, OR, USA) was used to evaluate the *in-situ* production of ROS. Freshly isolated vascular segments of cerebral arteries, incubated in DHE (5 μmol/L) for 1 hour in a light protected humidified chamber at 37°C were treated with or without 40 ng/mL insulin in the presence and absence of L-NAME (100 μmol/L), 7-NI (10 μmol/L), or sepiapterin (10 μmol/L). Then, the vascular segments were washed in phosphate-buffered saline and embedded in freezing medium (Optimal Cutting Temperature; Sakura Finetek USA, Torrance, CA, USA) and snap frozen in liquid nitrogen. Transverse sections (40 μm) of the arteries were cut with a cryostat (Leica CM 1850 UV Cryostat, Leica Microsystems, Germany), and mounted onto Superfrost Plus microscope slides. Fluorescence images of DHE were acquired using a Zeiss 7 Live laser scanning confocal microscope ($\lambda_{excitation}$ 488 nm and $\lambda_{emission}$ >560 nm) containing 40× 'Plan-Neofluar' objective with numerical aperture of 0.7. The presence of vascular ROS was revealed as red DHE fluorescence. Three to six sections of each vascular segment were imaged simultaneously from ZL and ZO rat pairs under identical conditions and microscopy settings. All images were analyzed offline using NIH-Image J application and presented as mean pixel intensity (arbitrary units) normalized to the fluorescence intensity of corresponding paired untreated ZL vascular section.

Average DHE fluorescence intensity for each animal represents the average fluorescence of all sections of the vascular segments imaged.

Insulin and Vascular Signaling

Isolated cerebral arteries were treated with and without insulin (40 ng/mL) in low glucose Dulbecco's Modified Eagle Medium medium at 37°C for 15 to 20 minutes. Arteries were washed and snap frozen in liquid nitrogen. Subsequently, homogenates were prepared from the tissues to determine the cellular signaling by western blotting.

RT-PCR

Total RNA was obtained from isolated cerebral arteries using the SV Total RNA Isolation System (Promega, Madison, WI, USA). RT-PCR experiments were performed in an Eppendorf Mastercycler thermocycler (Brinkmann Instruments, Westbury, NY, USA) as previously described (Katakam *et al*, 2006, 2009*a*). From each sample, 50 pg of total RNA was reverse transcribed and amplified using QIAGEN OneStep RT-PCR Kit with gene-specific primers targeting rat insulin receptor (sense primer: 5′-GCCATCCCGAAAGCGAAGATC-3′; anti-sense primer: 5′-TCTGGGTCCTGATTGCAT-3′; reference sequence NM_017071). Expected lengths of the RT-PCR product were 224 base pairs. We used 35 cycles for insulin receptor amplification. In control experiments, when reverse transcription was omitted, no amplification was observed.

Western Blot Analysis

Western blot analyses were performed as previously described (Katakam *et al*, 2009*a*, *b*). Briefly, equal amounts of extracted protein from homogenates of cerebral arteries were separated by 4% to 20% SDS-PAGE and transferred onto a nitrocellulose membrane (Bio-Rad, Hercules, CA, USA). Membranes were blocked with 1% nonfat milk in Tris-buffered saline and 0.05% Tween-20 for 1 hour at room temperature. Subsequently, the membranes were incubated overnight at 4°C with the primary antibodies for human insulin receptor β subunit (1:4,000; BD Transduction Laboratories, San Jose, CA, USA), total and phosphorylated endothelial NOS (eNOS) (1:4,000; BD Transduction Laboratories), total nNOS and inducible NOS (iNOS) (1:2,000; BD Transduction Laboratories), GTP-CH (1:500; Santa Cruz Biotechnology, Santa Cruz, CA, USA) total Akt (1:4,000; BD Transduction Laboratories), phosphorylated Akt that recognize the phosphorylated Ser473 (1:5,000; Cell Signaling Technology, Danvers, MA, USA), phosphorylated PKC-pan (1:2,500; Cell Signaling Technology), phosphorylated PKC-α/β (1:2,000; BD Transduction Laboratories), total and phosphorylated ERK-1/2 (1:2,500; Promega), and β-actin (1:2,500; Sigma). The membranes were then washed and for 2 hours in the blocking buffer with anti-rabbit IgG (1:50,000 dilution; Jackson ImmunoResearch, West Grove, PA, USA) conjugated to horseradish peroxidase. The final reaction products were visualized using enhanced chemiluminescence (SuperSignal West Pico; Pierce, Rockford, IL, USA) and recorded on X-ray film. Each immunoband intensity was normalized to the corresponding immunoband intensity of β-actin, which was used as a loading control.

Drugs, Chemicals, and Solutions

All chemicals were purchased from Sigma except MnTBAP (Calbiochem, San Diego, CA, USA) and DHE (Molecular Probes). Stock solutions of 7-NI and apocynin were prepared in dimethyl sulfoxide and all the other chemicals were prepared in deionized water. The composition of physiological salt solution (mmol/L) was NaCl (112), KCl (4.8), $NaHCO_3$ (26), $KH_2PO_4 \cdot H_2O$ (1.2), $CaCl_2$ (1.8), $MgSO_4 \cdot 7H_2O$ (1.2), and glucose (10). Physiological salt solution with 60 mmol/L KCl was prepared by replacing NaCl with an equimolar quantity of KCl.

Data Analysis and Statistics

All data are reported as mean ± s.e.m. '*n*' Indicates the number of independent experiments and also the number of animals used. Comparisons between the groups were performed by analysis of variance and *post hoc* analysis was performed by Student–Newman–Keuls method. A $P < 0.05$ was considered as statistically significant.

Results

Plasma Insulin and Glucose Measurements

Fasting plasma glucose levels (mg/dL) were 143 ± 8 in ZL rats ($n = 9$), 144 ± 10 in ZO rats ($n = 9$; $P =$ NS), 148 ± 8 in young SD rats ($n = 5$), and 137 ± 10 in aged SD rats ($n = 8$; $P =$ NS), indicating normoglycemia. Overall, the fasting glucose levels are slightly higher than 125 mg/dL as the blood samples were collected from anesthetized rats. In contrast, fasting plasma insulin levels (ng/mL) were significantly elevated in aged SD rats (2.5 ± 0.15, $n = 8$; $P < 0.05$) and in ZO rats (8.55 ± 0.59, $n = 9$; $P < 0.05$) compared with young SD rats (1.07 ± 0.08, $n = 5$) and ZL rats (1.9 ± 0.96, $n = 9$) respectively, confirming hyperinsulinemia and IR.

Expression of Insulin Receptor

Our previous study was the only report of the presence of insulin receptors in intact rat cerebral arteries. To confirm the presence of insulin receptors, we determined their expression in cerebral arteries of Zucker rats. PCR experiments showed the presence of 224 bp length insulin receptor mRNA in the rat cerebral arteries (Figure 1A). Similarly, the 95-kDa insulin receptor β subunit protein was also identified in the homogenates of rat cerebral arteries (Figure 1B).

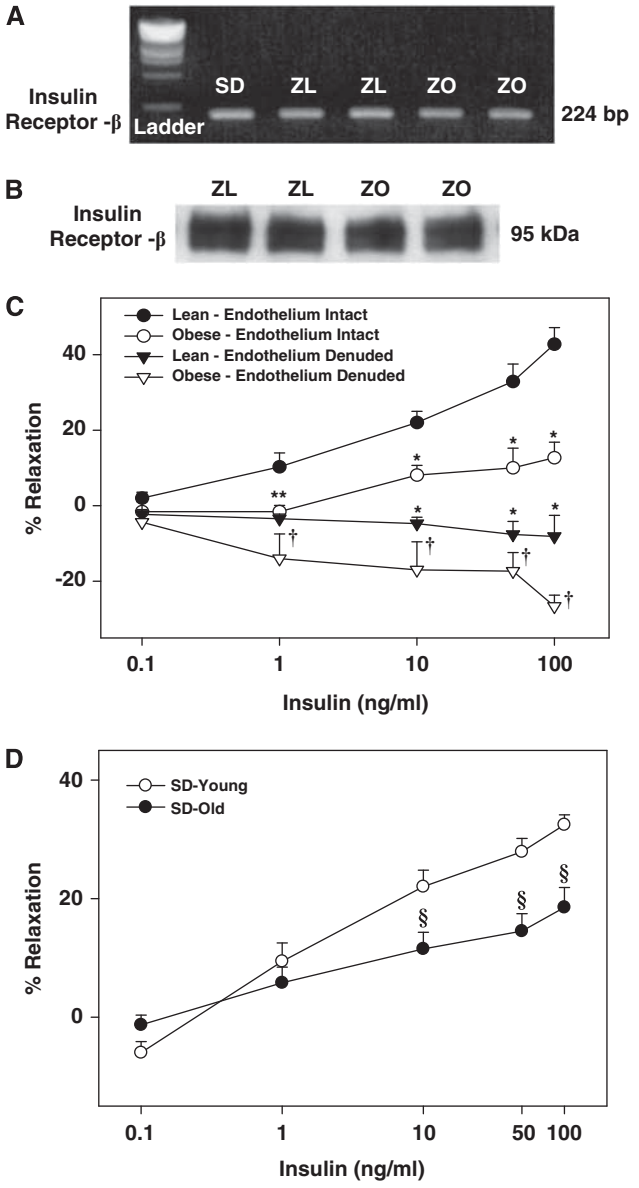

Figure 1 (**A**) The bands representing the PCR products of insulin receptor β in isolated cerebral arteries of Sprague-Dawley (SD), Zucker lean (ZL), and Zucker obese (ZO) rats are shown. (**B**) The immunobands identifying the insulin receptor β subunit in homogenates of cerebral arteries of ZL and ZO rats are shown. Vascular responses to insulin in grouped cerebral arteries of ZO and ZL rats with intact endothelium and endothelium denuded are shown in panel **C**. (**D**) Vascular responses to insulin in grouped cerebral arteries of younger and aged SD rats are shown. Data are mean ± s.e.m. of 6 to 12 experiments. (*) and (†) Indicate significant difference with respect to response to insulin in endothelium intact arteries of ZL and ZO rats, respectively ($P < 0.05$). (§) Indicate significant difference with respect to response to insulin in endothelium intact arteries of young SD rats ($P < 0.05$).

Insulin and Vasoreactivity

The average resting intraluminal diameter of cerebral arteries from all rats for each group of experiments was similar and they were preconstricted to a similar extent before the administration of various concentrations of insulin to determine the vasodilation elicited by insulin (online Supplementary Table 1). Insulin elicited a dose-dependent vasodilation in all cerebral arteries; however, significantly reduced vasodilation was observed in ZO compared with ZL rats (Figure 1C). Similarly, decreased insulin-induced vasodilation (% maximal vasodilation) was observed in the cerebral arteries of aged SD rats (19.7 ± 3, $n = 8$; $P < 0.05$) compared with arteries from young SD rats (32.0 ± 3, $n = 12$) (Figure 1D). Denudation of endothelium revealed a dose-dependent vasoconstriction to insulin in all arteries but ZO arteries displayed greater vasoconstriction (Figure 1C).

Inhibition of COX by indomethacin enhanced vasodilation in ZL arteries at low insulin concentrations although maximal vasodilation was unchanged (Figure 2A). In contrast, indomethacin enhanced vasodilation to all concentrations of insulin in ZO arteries ($n = 5$, $P < 0.05$, Figure 2A). Thus, insulin promoted significantly greater production of vasoconstrictor COX metabolites in ZO arteries. N^{ω}-nitro L-arginine methyl ester treatment resulted in diminished maximal relaxation to insulin in ZL arteries implicating nitric oxide (NO) in vasodilation (Figure 2B). In contrast, selective inhibition of nNOS with 7-NI had no impact on insulin-induced vasodilation in ZL arteries, suggesting that nNOS did not contribute NO. Paradoxically, L-NAME improved maximal vasodilation to insulin in ZO arteries, suggesting that NOS generates a vasoconstrictor factor, possibly ROS (Figure 2B). Interestingly, 7-NI also promoted vasodilation in ZO arteries, suggesting that nNOS also contributed to the vasoconstriction (Figure 2B). Sepiapterin pretreatment resulted in improvement of vasodilation to insulin only in ZO arteries indicating reduced BH_4 bioavailability, a known mechanism underlying NOS uncoupling. Sepiapterin has been shown to display nonspecific vascular actions. However, in the present study the vasoreactivity studies of arteries treated with sepiapterin indicate that the BH_4 bioavailability appeared to be unchanged in ZL rats (Figure 2C). Thus, at the dosage used and under the conditions of the present study sepiapterin displayed reasonable condition-specific selectivity in ZO arteries.

Inhibition of ROS generation with apocynin did not affect the maximal vasodilation to insulin in ZL arteries, whereas apocynin improved vasodilation in ZO arteries (Figure 3A). This indicates that insulin activated NADPH oxidase leading to excess ROS generation, which in turn diminished vasodilation to insulin in ZO arteries. However, in ZL arteries, insulin-induced ROS production by NADPH oxidase was not sufficient to alter the vasodilation. Scavenging of the ROS with PEG-SOD improved vasodilation to 1 ng/mL insulin in ZL arteries compared with baseline although maximal relaxation to insulin was unchanged, indicating that insulin promotes ROS generation at basal levels that oppose the vasodilator response to insulin. In ZO arteries, however, PEG-

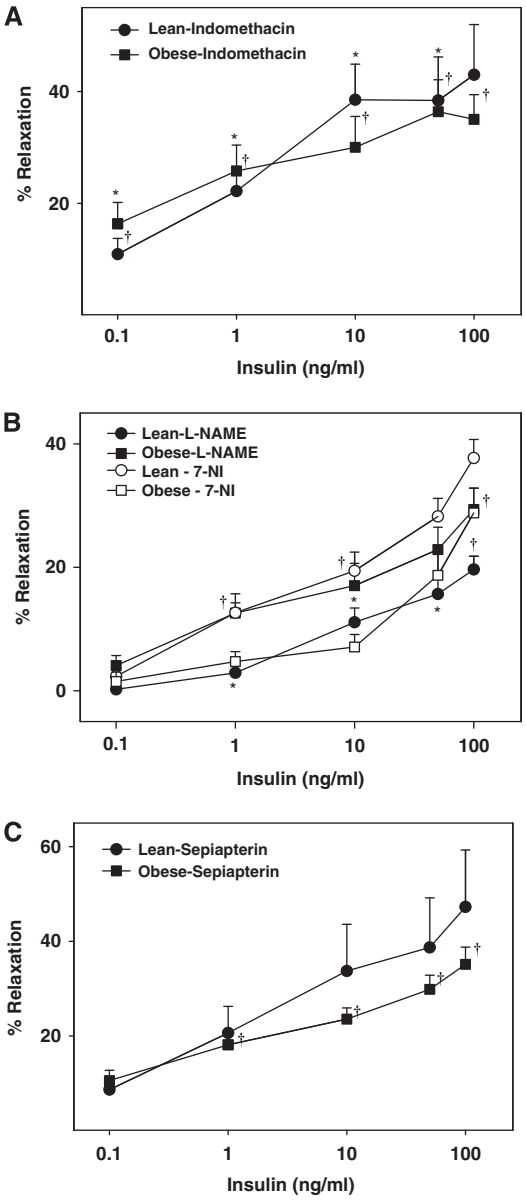

Figure 2 Vascular responses to insulin in cerebral arteries of Zucker obese (ZO) and Zucker lean (ZL) with intact endothelium, in the presence of indomethacin (**A**), N^{ω}-nitro L-arginine methyl ester (L-NAME) and 7-nitroindazole (7-NI) (**B**), and sepiapterin (**C**) are shown. Data are mean ± s.e.m. of 5 to 8 experiments. (*) and (†) Indicate significant difference with respect to insulin response in untreated arteries of ZL and ZO rats, respectively ($P < 0.05$).

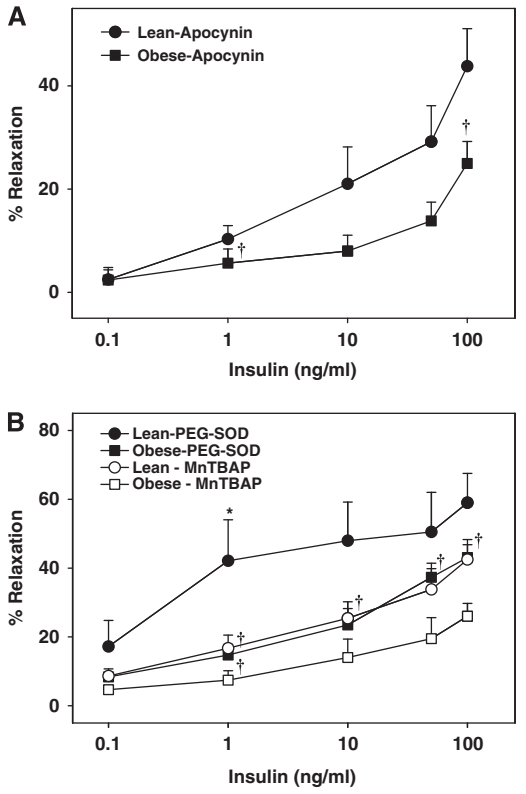

Figure 3 Vascular responses to insulin in cerebral arteries of Zucker obese (ZO) and Zucker lean (ZL) with intact endothelium, in the presence of apocynin (**A**), poly-ethylene glycol-superoxide dismutase (PEG-SOD) and manganese(III) tetrakis(4-benzoic acid)porphyrin chloride (MnTBAP) (**B**) are shown. Data are mean ± s.e.m. of 4 to 8 experiments. (*) and (†) Indicate significant difference with respect to insulin response in untreated arteries of ZL and ZO rats, respectively ($P < 0.05$).

SOD treatment normalized the vasodilation indicating that increased oxidative stress diminished vasodilation in ZO arteries (Figure 3B). In addition, scavenging of the ROS with MnTBAP did affect the vasodilation to insulin in ZL arteries whereas MnTBAP promoted vasodilation in ZO arteries (Figure 3B).

Pretreatment with L-NAME and 7-NI constricted the arteries in all rats; however, ZO arteries exhibited increased constriction to L-NAME compared with ZL arteries. Pretreatment with indomethacin dilated all arteries whereas pretreatment with sepiapterin, apocynin, PEG-SOD, and MnTBAP had no effect on baseline diameter of the arteries.

Vascular Signaling

Cellular kinases mediate vasodilator and vasoconstrictor signaling in arteries. To uncover the signaling mechanisms underlying the impaired vascular actions of insulin in IR, we determined the activation of the key kinases and their targets known to regulate vasoreactivity. Treatment of rat cerebral arteries with insulin *in vitro* elicited phosphorylation of kinases in all arteries. Zucker obese arteries exhibited diminished insulin-induced phosphorylation of eNOS compared with ZL arteries (Figure 4A). However, insulin did not affect the expression of total eNOS, nNOS, or iNOS in all arteries (Figures 4A and 4B). Total expression of eNOS was enhanced in ZO arteries at baseline compared with ZL arteries, indicating a possible response to reduced NO bioavailability. In addition, ZO arteries displayed

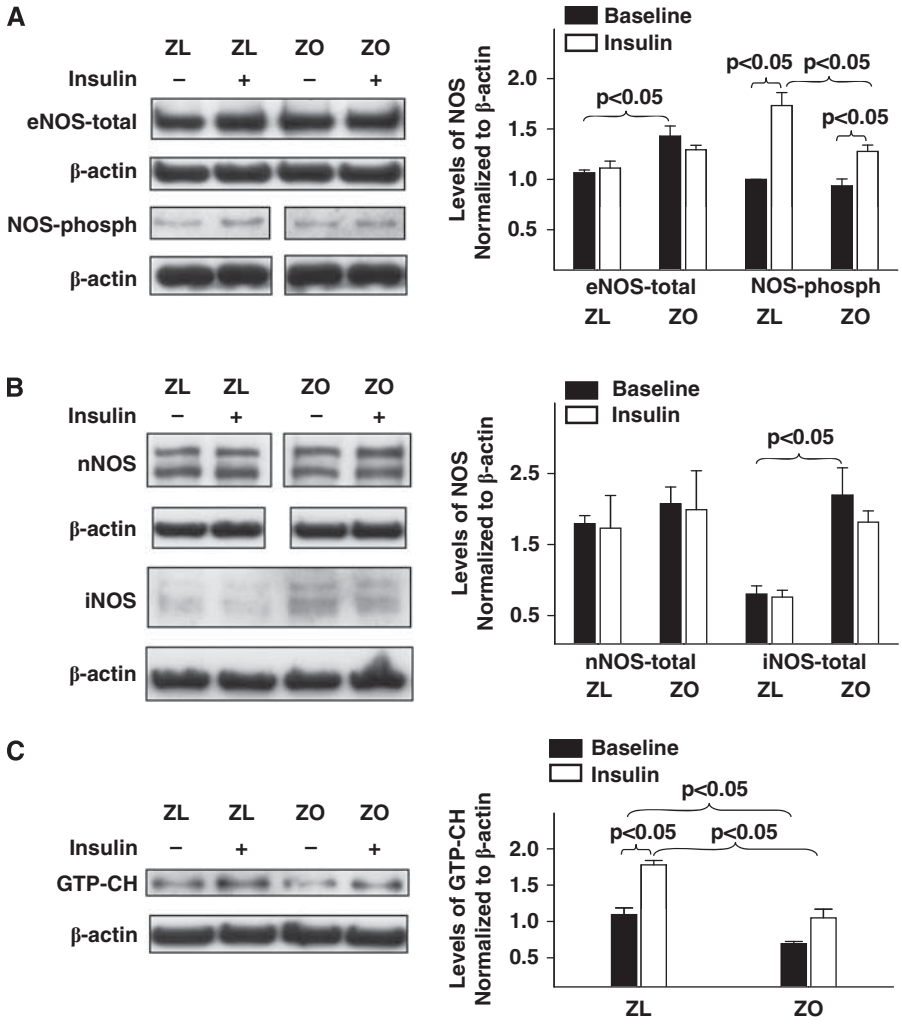

Figure 4 Representative immunoblots of homogenates of Zucker obese (ZO) and Zucker lean (ZL) cerebral arteries treated with or without insulin for 15 to 20 minutes at 37°C are shown. Immunoblots of total and phosphorylated endothelial nitric oxide synthase (eNOS) (**A**), neuronal NOS (nNOS) and inducible NOS (iNOS) (**B**), and GTP cyclohydrolase-I (GTP-CH) (**C**) with corresponding β-actin immunoblots are shown. Representative images of western blots of phosphorylated eNOS and nNOS along with corresponding β-actin immunoblots are shown from different parts of the same gels. Zucker lean and ZO group data from 3 to 5 animals each are mean ± s.e.m. of immunoband intensity in arbitrary units normalized to β-actin and are represented as bar graphs on the right side.

increased iNOS expression at baseline, suggesting an underlying vascular inflammatory process. Inducible NOS immunobands from protein extracts of ZL arteries were barely visible indicating lack of expression (Figure 4B). Expression of GTP-CH at basal levels was diminished in ZO arteries compared with ZL arteries. Treatment with insulin enhanced the expression of GTP-CH in all arteries although ZO arteries exhibited diminished increase in GTP-CH expression compared with ZL arteries. Taken together, it appears that ZO arteries have a reduced ability to regenerate BH_4 at baseline and in response to insulin (Figure 4C). Insulin treatment of arteries increased the phosphorylation of Akt without changing the total Akt; however, the Akt phosphorylation was diminished in ZO arteries compared with ZL arteries (Figure 5A). In contrast, insulin-induced phosphorylations of pan-PKC, PKC-α/β, and ERK 1/2 were increased in ZO compared with ZL arteries (Figures 5B and 5C).

Reactive Oxygen Species Generation

Fluorescence microscopy revealed greater DHE fluorescence in ZO than in ZL arterial sections, indicating increased ROS production under baseline conditions (Figures 6A, 6B, and 6G). In ZL arteries, L-NAME enhanced DHE fluorescence compared with the untreated arteries suggesting that NO may reduce ROS (Figures 6C and 6G). In contrast, treatment with 7-NI did not change the DHE fluorescence in ZL arteries, indicating that nNOS had no impact on vascular ROS (Figure 6G). Paradoxically, in ZO

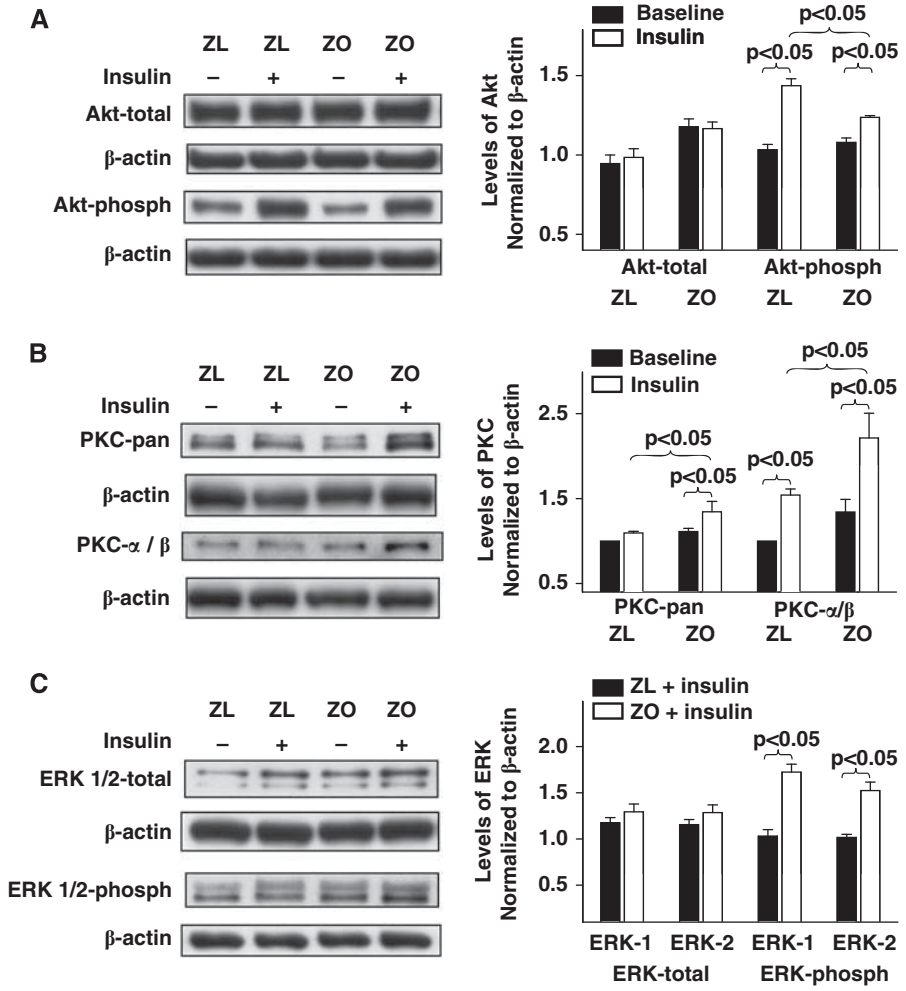

Figure 5 Representative immunoblots of homogenates of Zucker obese (ZO) and Zucker lean (ZL) cerebral arteries treated with or without insulin for 15 to 20 minutes 37°C are shown. Immunoblots of total and phosphorylated Akt (**A**), phosphorylated PKC-pan and PKC-α/β (**B**), total and phosphorylated ERK 1/2 (**C**) with corresponding β-actin immunoblots are shown. Group data from 3 to 5 animals each are mean ± s.e.m. of immunoband intensity in arbitrary units normalized to β-actin and are represented as bar graphs on the right side. Akt-phosph, phosphorylated Akt; ERK-phosph, phosphorylated ERK.

arteries, L-NAME and 7-NI diminished DHE fluorescence implying that part of the ROS probably originated from uncoupled NOS isoforms including nNOS. This indicates the ability of insulin to promote ROS generation independent of its ability to stimulate NO production. In ZL arteries, combined treatment with L-NAME and insulin enhanced the DHE fluorescence more than when each treatment was applied alone. This implies an additive effect of diminished NO mediated ROS reduction and increased generation of ROS. In contrast, combined treatment with 7-NI and insulin did not increase the DHE fluorescence in ZL arteries, indicating that nNOS was not a source of insulin-induced ROS generation (Figure 6G). Paradoxically, in ZO arteries, both L-NAME and 7-NI co-treatment with insulin abolished insulin-induced increases in DHE fluorescence suggesting that uncoupled NOS isoforms, including eNOS/iNOS and nNOS, generated ROS in response to insulin (Figures 6D, 6F, and 6G). Furthermore, sepiapterin treatment diminished the enhanced DHE fluorescence at baseline and in response to insulin in ZO arteries implicating reduced BH_4 bioavailability in NOS uncoupling (Figures 6E and 6G).

Discussion

The present study reports impaired cerebrovascular actions of insulin in diabetes or IR. We show that cerebral vascular responsiveness to insulin is reduced in IR animals associated with obesity due to complex changes in vasodilation and vasoconstriction pathways based on the following original findings: (1) insulin-induced vasodilation in isolated cerebral arteries was significantly diminished in ZO rats compared with ZL rats; (2) eNOS-derived NO mediated insulin-induced vasodilation in ZL arteries

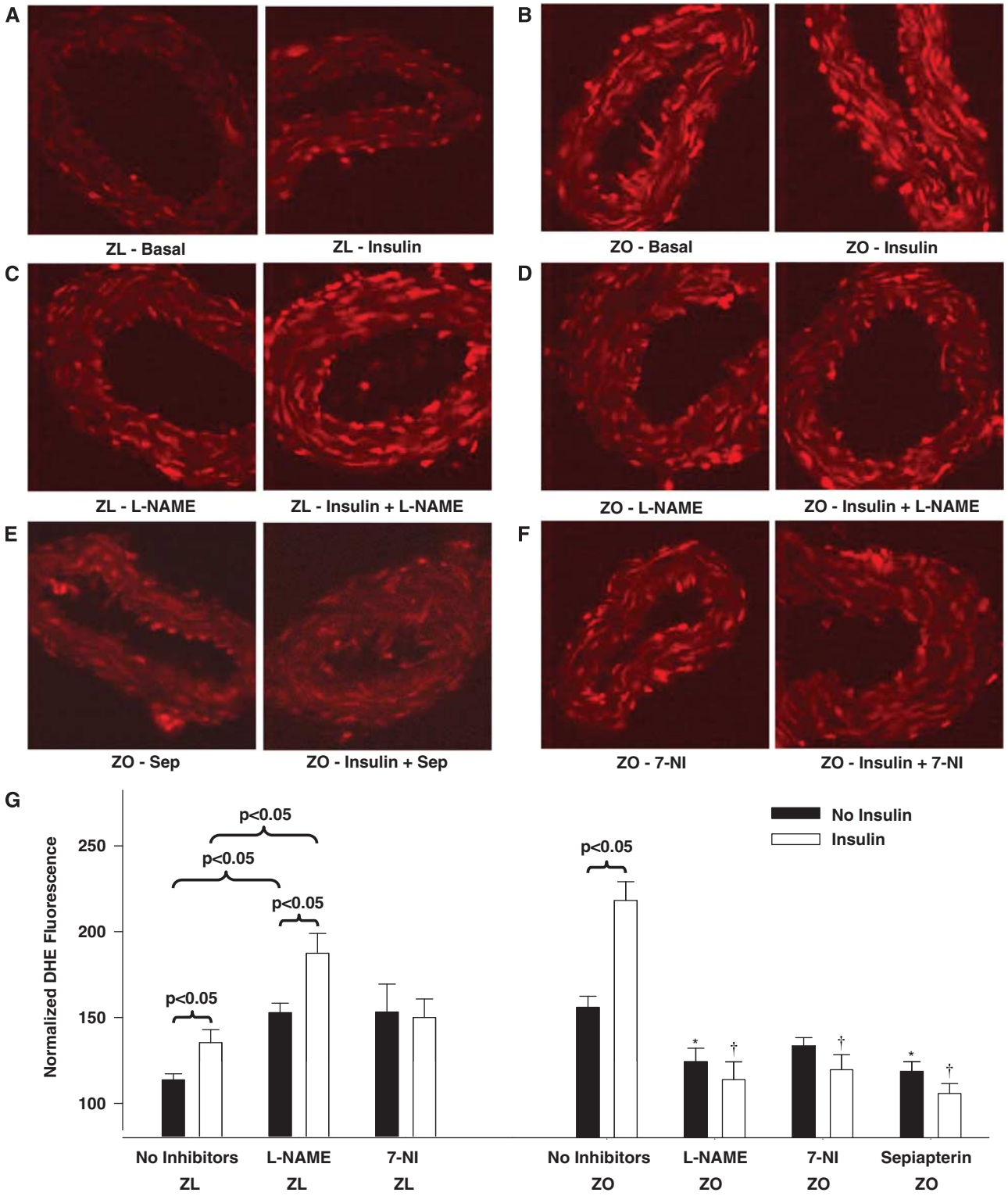

Figure 6 Representative dihydroethidium (DHE) fluorescence images of sections of Zucker obese (ZO) and Zucker lean (ZL) cerebral arteries treated with or without insulin are shown. Fluorescence images of ZL arterial sections acquired at baseline or after insulin treatment in the absence (**A**) or presence of N^{ω}-nitro L-arginine methyl ester (L-NAME) (**C**) are shown. Fluorescence images of ZO arterial sections acquired at baseline or after insulin treatment in the absence (**B**) or presence of L-NAME (**D**) or sepiapterin (Sep, **E**) or 7-nitroindazole (7-NI) (**F**) are shown. Group data from 3 to 5 animals each are expressed as mean ± s.e.m. of normalized fluorescence intensity in arbitrary units and are represented as bar graph (**G**). (*) and (†) Indicate significant difference with respect to DHE fluorescence in ZO arteries at baseline or after insulin treatment in the absence of any inhibitors, respectively ($P < 0.05$).

whereas in ZO arteries, NO-mediated vasodilation was lost and uncoupling of NOS isoforms resulted in ROS generation contributing to vasoconstriction. Supplementation with the precursor of BH_4 diminished the insulin-induced ROS generation and restored vasodilation in ZO arteries implicating NOS uncoupling in cerebrovascular IR; (3) ZO arteries exhibited decreased expression of GTP-CH at baseline and after insulin treatment compared with ZL arteries that contributed to the reduced BH_4 bioavailability; (4) insulin promoted abnormal activation of NADPH oxidase in ZO arteries leading to increased generation of ROS and diminished vasodilation. Scavenging of ROS or inhibition of NOS isoforms partially restored insulin-induced vasodilation in ZO arteries confirming the role of oxidative stress in cerebrovascular IR; (5) COX metabolites primarily mediated vasoconstriction in response to insulin and increased production of vasoconstrictor prostanoids reduced vasodilation to insulin in ZO arteries; (6) abnormal insulin-induced phosphorylation of kinases resulted in diminished vasodilatory (eNOS and Akt) and enhanced vasoconstrictor (pan-PKC, PKC-α/β, and ERK-1/2) signaling in ZO arteries. Thus, taken together, these findings show that cerebrovascular IR in ZO rats displays selective resistance to signaling pathways that promote vasodilation compounded by selective promotion of vascular signaling that induce vasoconstriction as summarized in the schematic in Figure 7.

Our laboratory identified the mRNA and protein of insulin receptors in the cerebral arteries of SD rats (Katakam *et al*, 2009*a*). In the present study, we identified mRNA and protein of insulin receptors in the cerebral arteries of Zucker rats comparable in size to the insulin receptors previously reported (Katakam *et al*, 2009*a*; Moloney *et al*, 2010).

Normal fasting plasma insulin levels in humans are < 1 ng/mL and they are elevated many times over the basal levels after ingesting a meal; however, obese humans display insulin levels often 3 to 5 times higher at fasting and postprandial states (Polonsky *et al*, 1988). Moreover, a person with diabetes receiving NovoLog insulin injections

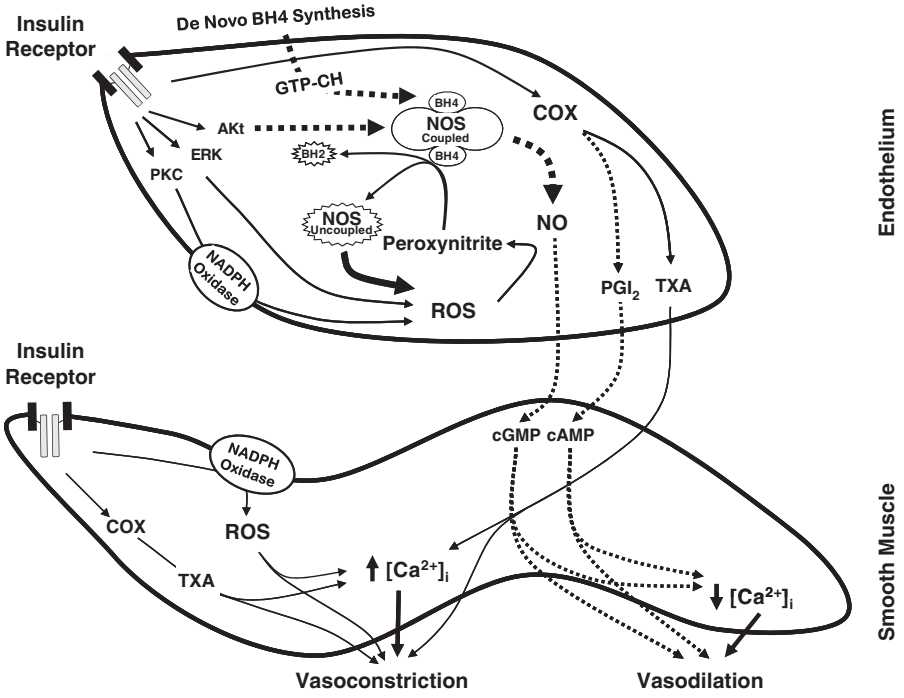

Figure 7 A schematic of the mechanisms underlying cerebrovascular insulin resistance (IR) in Zucker obese (ZO) rats. Insulin binding to insulin receptor leads to activation of kinase signaling by phosphorylation that in turn activates downstream signaling pathways. Zucker obese arteries displayed reduced phosphorylation of Akt and its target, endothelial nitric oxide synthase (eNOS), resulting in diminished nitric oxide (NO)-mediated vasodilation. Insulin binding also resulted in enhanced PKC and ERK 1/2 phosphorylation and activation in ZO arteries that may likely mediate excess superoxide production by NADPH oxidase. Excessive reactive oxygen species (ROS) formation in response to insulin in ZO arteries promoted enhanced vasoconstriction that was reversed by the scavenging of ROS. In addition, oxidative stress in ZO arteries may have induced uncoupling of NOS by oxidation of tetrahydrobiopterin (BH_4), an essential cofactor for the activation of NOS that stabilizes the dimeric form of the enzyme, leading to superoxide formation. Zucker obese arteries also displayed decreased expression of GTP cyclohydrolase-I (GTP-CH), a rate-limiting enzyme in the *de-novo* biosynthesis of BH_4, at baseline and in response to insulin, which further impairs their ability to regenerate BH_4 in the context of increased oxidative degradation of BH_4. Zucker obese arteries also exhibit enhanced vasoconstriction mediated by cyclooxygenase (COX) metabolites. Thus, cerebrovascular IR in ZO arteries is characterized by depressed activation (dotted arrows) of vasodilatory and exaggerated activation (solid arrows) of vasoconstrictor pathways. PGI_2, prostaglandin I_2; TXA, thromboxane.

(1 unit/kg per day) may display plasma insulin levels of 10 ng/mL or higher (prescribing information of Novo Nordisk, Princeton, NJ, USA), based on the WHO established standard (WHO Expert Committee on Biological Standardization. Thirty-Seventh Report, 1987). In the present study, insulin concentrations ranged from 0.1 to 100 ng/mL and thus covered physiological, pathological, and pharmacological insulin levels.

Cerebrovascular Insulin Resistance Accompanies Metabolic Insulin Resistance

Zucker obese rats and aged SD rats displayed similar plasma glucose levels but hyperinsulinemia when compared with their respective controls, ZL rats and younger SD rats confirming obesity and age-related metabolic IR with normoglycemia. Consistent with our previous observations in SD rats (Katakam *et al*, 2009*a*), insulin induced vasodilation in isolated cerebral arteries of Zucker rats. However, the vasodilation to insulin was diminished in ZO compared with ZL rats signifying cerebrovascular IR. Similarly, insulin-induced vasodilation was also reduced in aged SD rats compared with younger SD rats. Thus, cerebrovascular IR accompanied metabolic IR in two diverse models of IR, indicating that vascular IR observed was independent of underlying etiology of IR.

Vasodilation elicited by insulin was entirely endothelium-dependent but endothelial denudation abolished vasodilation, and instead revealed dose-dependent vasoconstriction to insulin. This vasoconstrictor response to insulin was enhanced in ZO arteries compared with ZL arteries. Thus, reduced vasodilation combined with enhanced vasoconstriction underlies the cerebrovascular IR in ZO arteries.

Role of Cyclooxygenase

Consistent with our previous studies (Katakam *et al*, 2009*a*), activation of COX by insulin promoted the generation of vasoconstrictor metabolites from the vascular wall in Zucker rats. Cerebral arteries of ZO rats appeared to produce increased vasoconstrictor prostanoids in response to insulin, leading to greater vasoconstriction compared with ZL arteries. Similar abnormal activation of COX in response to insulin has also been implicated in vascular dysfunction in T2DM (Bagi *et al*, 2005).

Role of Nitric Oxide Synthase Uncoupling

Insulin-induced vasodilation in ZL arteries was mediated primarily by NO originating only from eNOS, unlike SD rat cerebral arteries where both eNOS and nNOS participated in vasodilation (Katakam *et al*, 2009*a*). We previously observed that NO-mediated vasodilation was diminished in ZO arteries despite the evidence of increased eNOS and iNOS expression compared with ZL arteries (Erdos *et al*, 2004; Katakam *et al*, 2009*b*). Moreover, a reduced phosphorylated NOS protein in response to insulin, consistent with reduced NO-mediated vasodilation, was observed in ZO arteries compared with ZL arteries. Interestingly, NOS appears to release a vasoconstrictor factor in response to insulin in ZO arteries since inhibition of NOS paradoxically promoted vasodilation. It is known that NOS isoforms in an uncoupled state produce superoxide anion, which promotes vasoconstriction by direct activation of vasoconstrictor pathways or by decreasing the NO bioavailability. Inhibition of all NOS isoforms, or specifically nNOS, partially restored the insulin-induced vasodilation implicating uncoupling of NOS isoforms and subsequent superoxide anion production in the diminished vasodilation. Indeed, direct ROS measurement confirmed enhanced ROS production in ZO arteries in response to insulin that was partially restored by BH_4 precursor supplementation or inhibition of NOS in general and nNOS in particular. Western blot studies identified all three isoforms of NOS in cerebral arteries of Zucker rats. Thus, uncoupling of NOS in ZO arteries may likely involve all NOS isoforms.

Reduced Tetrahydrobiopterin Bioavailability and GTP Cyclohydrolase-I Expression

Tetrahydrobiopterin is a cofactor regulating NOS activity and NO synthesis by promoting eNOS dimerization and protein stability. Reduced BH_4 levels promote eNOS uncoupling leading to formation of superoxide (Katusic *et al*, 2009; Tarpey, 2002). In endothelial cells, reduction of BH_4 levels occurs due to either increased oxidative conversion to 7,8-dihydrobiopterin (BH_2) or decreased biosynthesis by GTP-CH, a rate-limiting enzyme in the *de-novo* biosynthesis of BH_4 (Katusic *et al*, 2009). Indeed, we made a novel observation that GTP-CH expression was diminished in ZO arteries at baseline and after activation with insulin compared with ZL arteries. Reduced GTP-CH expression has been shown in type 1 diabetes (Wang *et al*, 2009) but reduced GTP-CH expression in the absence of hyperglycemia in IR in ZO rats is a novel finding. Similarly, insulin's ability to enhance the expression of GTP-CH in cerebral arteries is consistent with previous report (Ishii *et al*, 2001). Importantly, sepiapterin treatment to promote increased BH_4 generation improved the vasodilation to insulin in ZO rats suggesting decreased BH_4 bioavailability. Conflicting findings have been reported showing sepiapterin improved (Laursen *et al*, 2001; Shinozaki *et al*, 2000) or worsened (Mitchell *et al*, 2004) the diminished vasodilation in conditions with uncoupled eNOS. Sepiapterin has been shown to display many actions and the effects of sepiapterin may be the result of the extent of BH_4 salvage pathway activity and conversion to BH_4 as well as sepiapterin binding to eNOS in competition with BH_4. In addi-

tion, BH_4 bioavailability is dependent on the rate of autoxidation and consumption by reacting to peroxynitrite. It has been suggested that the ratio of reduced and oxidized biopterin may be physiologically important in determining the rates of NO production versus uncoupled superoxide formation from eNOS (Tarpey, 2002). However, under our experimental conditions, ROS measurements confirmed that sepiapterin indeed diminished insulin-induced ROS generation in ZO arteries. Thus, the demonstration of insulin's ability to induce uncoupling of NOS isoforms is a novel observation of the present study.

Role of Oxidative Stress

Reduced BH_4 levels due to oxidative degradation of BH_4 to BH_2 has been reported in diabetes (Shinozaki *et al*, 2000). Furthermore, BH_2 competes for binding to NOS at the BH_4 site, thus promoting NOS uncoupling and loss of NO production (Katusic *et al*, 2009). Increased ROS production in ZO arteries is an additional mechanism underlying the uncoupling of NOS by oxidative degradation of BH_4 to BH_2. Increased vasoconstriction and reduced vasodilation in ZO arteries in response to insulin also appear to be mediated by ROS because scavenging the ROS with PEG-SOD or MnTBAP or inhibition of ROS generation with apocynin, L-NAME, or 7-NI promoted vasodilation. Interestingly, the ROS scavengers, PEG-SOD and MnTBAP, displayed variable degree of effect on insulin-induced vasodilation in Zucker arteries. This finding may be explained by their differences in molecular structure, intracellular distribution, and mechanisms of scavenging. Alternatively, MnTBAP has been proposed to be relatively more efficient scavenger of mitochondrial ROS than SOD (Patel, 2003; Szabo *et al*, 1996); thus, it may be speculated that insulin promoted mitochondrial dysfunction in the arterial wall by activating mitochondrial ROS generation in ZO arteries. However, further studies are required to establish direct activation of mitochondrial oxidative stress by insulin in ZO arteries.

Consistent with our previous observations in coronary arteries (Katakam *et al*, 2005), direct measurements of ROS showed the ability of insulin to activate ROS production in rat cerebral arteries. Overall, ROS generation at basal and insulin activated states was greatly increased in ZO arteries. Importantly, ROS generation in ZO arteries was diminished by NOS inhibition or promoting BH_4 generation supporting the role of NOS uncoupling in cerebrovascular IR. Surprisingly, NOS inhibition in ZL arteries enhanced vascular ROS. It is not clear whether NO simply quenches ROS or exhibits more complex regulation of ROS generation. In addition to uncoupling of NOS, enhanced insulin-induced activation of NADPH oxidase appears to contribute to the oxidative stress in ZO arteries as inhibition of NADPH oxidase activity partially restored the cerebrovascular vasodilation in ZO rats. We reported similar observations related to coronary vascular dysfunction in ZO rats (Katakam *et al*, 2005). It has been proposed that in endothelial cells and vascular smooth muscle cells, apocynin reduces ROS not by inhibiting NAPDH oxidase but possibly by scavenging ROS (Heumuller *et al*, 2008). However, it has been argued that whether apocynin inhibits NADPH oxidase in nonphagocytic cells without myeloperoxidase depends on the cell type studied and the ability of vascular wall to activate apocynin (Touyz, 2008). Insulin-induced vasodilation was improved by apocynin only in ZO arteries, suggesting that insulin enhanced NADPH oxidase activity in ZO arteries. Thus, the present study identified insulin as a novel instigator of NOS uncoupling in cerebrovascular IR via abnormal activation of NADPH oxidase.

Abnormal Vascular Signaling

Insulin elicited phosphorylation of Akt at ser473 in cerebral arteries of Zucker rats consistent with previous observations (Katakam *et al*, 2009*a*). Akt phosphorylation has been linked to phosphorylation of eNOS at Ser1177 and NO formation (Mount *et al*, 2007). Insulin also has been shown to stimulate NO synthesis by Akt-mediated phosphorylation and activation of eNOS (Ritchie *et al*, 2010). Cerebral arteries of Zucker rats also exhibited insulin-induced eNOS phosphorylation at Ser1177. However, phosphorylation of both Akt and eNOS in response to insulin was diminished in ZO compared with ZL arteries. As previously reported (Bakker *et al*, 2008*b*), insulin also induced phosphorylation of PKC (pan and α/β isoforms) in cerebral arteries. Enhanced PKC activation has been shown to promote vasoconstriction in ZO rats (Erdos *et al*, 2004) and models of T2DM (Bakker *et al*, 2008*a*) via activation of NADPH oxidase, promoting endothelin-1 expression and increasing mitochondrial ROS formation (Geraldes and King, 2010). We observed increased insulin-induced phosphorylation of PKC isoforms in ZO that may have contributed to the cerebrovascular IR. Finally, insulin has also been shown to activate ERK 1/2 signaling in vasculature that contributes to vasoconstrictor actions of insulin (Bakker *et al*, 2008*a*; Eringa *et al*, 2004). Cerebral arteries of Zucker rats similarly exhibited activation of ERK 1/2 by phosphorylation, which was greater in ZO arteries compared with ZL arteries. Thus, investigation of kinase signaling in the vascular wall revealed complex activation of pathways leading to impaired vasodilation and enhanced vasoconstriction.

Insulin Versus Other Vasodilators

Cerebrovascular actions of insulin in Zucker rats were unique when compared with other vasodilators. For example, previous studies in our laboratory showed that inhibition of NOS diminished vasodilation in cerebral arteries of ZL arteries in response

to two mechanistically different vasodilators, acetylcholine and diazoxide (Erdos *et al*, 2004; Katakam *et al*, 2009*b*). Unlike insulin, neither acetylcholine nor diazoxide improved vasodilation to insulin in ZO arteries in the presence of NOS inhibitors, suggesting that insulin displays unique ability to promote NOS uncoupling in IR (Erdos *et al*, 2004; Katakam *et al*, 2009*b*). In addition, we observed the ability to modulate expression of GTP-CH enzyme and activity of NOS isoforms unique to insulin. Thus, the present study uncovered unique vascular actions of insulin in cerebral arteries of ZO rats that have not been reported in other circulations such as mesenteric (Miller *et al*, 2002) or coronary (Katakam *et al*, 2005). It is noted that vasodilation to nitroprusside was unchanged in ZO arteries compared with ZL arteries (Erdos *et al*, 2004).

Limitations

It is acknowledged that our observations in ZO rats are confounded by the effects of obesity and leptin receptor mutation on the same signaling pathways affected by insulin. However, the significant distinction displayed by insulin in inducing NOS uncoupling in ZO arteries compared with many vasodilators we previously studied (Erdos *et al*, 2004; Katakam *et al*, 2005, 2009*b*) assures the specificity of insulin's action in cerebrovascular IR. Although it has been reported that hyperleptinemia has been associated with increased eNOS expression and uncoupling (Korda *et al*, 2008); hyperleptinemia has not been shown to directly stimulate NOS uncoupling. Moreover, the demonstration of cerebrovascular IR in aging-associated IR supports the argument that the obesity/leptin receptor mutation is unlikely to directly account for the impaired vascular actions of insulin in ZO rats.

Perspective

In conclusion, we showed that cerebrovascular IR accompanies metabolic IR in ZO rats. Diminished NO generation compounded by the increased oxidative stress resulting from NOS uncoupling and abnormal NADPH oxidase activity underlie the cerebrovascular IR. Inability of insulin to enhance GTP-CH and increased oxidative degradation of BH_4 may have contributed to reduced BH_4 bioavailability in IR. These observations have contributed to a paradigm whereby excessive ROS production in ZO arteries decreased bioavailability of NO and BH_4 leading to eNOS uncoupling and further formation of ROS, thus perpetuating a cycle of vascular oxidative stress in cerebrovascular IR.

Acknowledgements

The authors thank Nancy Busija for the help with editing the manuscript. The authors also acknowledge the help with immunostaining and fluorescence imaging of insulin receptors by Dr Edina A Wappler and Dr Paige S Katz.

Disclosure/conflict of interest

The authors declare no conflict of interest.

References

Bagi Z, Erdei N, Toth A, Li W, Hintze TH, Koller A, Kaley G (2005) Type 2 diabetic mice have increased arteriolar tone and blood pressure: enhanced release of COX-2-derived constrictor prostaglandins. *Arterioscler Thromb Vasc Biol* 25:1610–6

Bakker W, Eringa EC, Sipkema P, van Hinsbergh VW (2008*a*) Endothelial dysfunction and diabetes: roles of hyperglycemia, impaired insulin signaling and obesity. *Cell Tissue Res* 335:165–89

Bakker W, Sipkema P, Stehouwer CD, Serne EH, Smulders YM, van Hinsbergh VW, Eringa EC (2008*b*) Protein kinase C theta activation induces insulin-mediated constriction of muscle resistance arteries. *Diabetes* 57:706–13

Bray GA (1977) The Zucker-fatty rat: a review. *Fed Proc* 36:148–53

Center for Disease Control and Prevention. National Diabetes Fact Sheet, 2011 (2011) http://www.cdc.gov/diabetes/pubs/factsheet11.htm

Chen YL, Messina EJ (1996) Dilation of isolated skeletal muscle arterioles by insulin is endothelium dependent and nitric oxide mediated. *Am J Physiol* 270:H2120–4

Erdos B, Snipes JA, Miller AW, Busija DW. (2004) Cerebrovascular dysfunction in Zucker obese rats is mediated by oxidative stress and protein kinase C. *Diabetes* 53:1352–9

Erdos B, Snipes JA, Tulbert CD, Katakam P, Miller AW, Busija DW (2006) Rosuvastatin improves cerebrovascular function in Zucker obese rats by inhibiting NAD(P)H oxidase-dependent superoxide production. *Am J Physiol Heart Circ Physiol* 290:H1264–70

Eringa EC, Stehouwer CD, Merlijn T, Westerhof N, Sipkema P (2002) Physiological concentrations of insulin induce endothelin-mediated vasoconstriction during inhibition of NOS or PI3-kinase in skeletal muscle arterioles. *Cardiovasc Res* 56:464–71

Eringa EC, Stehouwer CD, van Nieuw Amerongen GP, Ouwehand L, Westerhof N, Sipkema P (2004) Vasoconstrictor effects of insulin in skeletal muscle arterioles are mediated by ERK1/2 activation in endothelium. *Am J Physiol Heart Circ Physiol* 287:H2043–8

Geraldes P, King GL (2010) Activation of protein kinase C isoforms and its impact on diabetic complications. *Circ Res* 106:1319–31

Heumuller S, Wind S, Barbosa-Sicard E, Schmidt HH, Busse R, Schroder K, Brandes RP (2008) Apocynin is not an inhibitor of vascular NADPH oxidases but an antioxidant. *Hypertension* 51:211–7

Ishii M, Shimizu S, Nagai T, Shiota K, Kiuchi Y, Yamamoto T (2001) Stimulation of tetrahydrobiopterin synthesis induced by insulin: possible involvement of phosphatidylinositol 3-kinase. *Int J Biochem Cell Biol* 33:65–73

Katakam PV, Domoki F, Lenti L, Gaspar T, Institoris A, Snipes JA, Busija DW (2009*a*) Cerebrovascular

responses to insulin in rats. *J Cereb Blood Flow Metab* 29:1955–67

Katakam PV, Domoki F, Snipes JA, Busija AR, Jarajapu YP, Busija DW (2009*b*) Impaired mitochondria-dependent vasodilation in cerebral arteries of Zucker obese rats with insulin resistance. *Am J Physiol Regul Integr Comp Physiol* 296:R289–98

Katakam PV, Snipes JA, Tulbert CD, Mayanagi K, Miller AW, Busija DW (2006) Impaired endothelin-induced vasoconstriction in coronary arteries of Zucker obese rats is associated with uncoupling of [Ca2+]i signaling. *Am J Physiol Regul Integr Comp Physiol* 290:R145–53

Katakam PV, Tulbert CD, Snipes JA, Erdos B, Miller AW, Busija DW (2005) Impaired insulin-induced vasodilation in small coronary arteries of Zucker obese rats is mediated by reactive oxygen species. *Am J Physiol Heart Circ Physiol* 288:H854–60

Katusic ZS, d'Uscio LV, Nath KA (2009) Vascular protection by tetrahydrobiopterin: progress and therapeutic prospects. *Trends Pharmacol Sci* 30:48–54

Korda M, Kubant R, Patton S, Malinski T (2008) Leptin-induced endothelial dysfunction in obesity. *Am J Physiol Heart Circ Physiol* 295:H1514–21

Laursen JB, Somers M, Kurz S, McCann L, Warnholtz A, Freeman BA, Tarpey M, Fukai T, Harrison DG (2001) Endothelial regulation of vasomotion in apoE-deficient mice: implications for interactions between peroxynitrite and tetrahydrobiopterin. *Circulation* 103:1282–8

Matsumoto K, Miyake S, Yano M, Ueki Y, Miyazaki A, Hirao K, Tominaga Y (1999) Insulin resistance and classic risk factors in type 2 diabetic patients with different subtypes of ischemic stroke. *Diabetes Care* 22:1191–5

Miller AW, Tulbert C, Puskar M, Busija DW (2002) Enhanced endothelin activity prevents vasodilation to insulin in insulin resistance. *Hypertension* 40:78–82

Mitchell BM, Dorrance AM, Ergul A, Webb RC (2004) Sepiapterin decreases vasorelaxation in nitric oxide synthase inhibition-induced hypertension. *J Cardiovasc Pharmacol* 43:93–8

Moloney AM, Griffin RJ, Timmons S, O'Connor R, Ravid R, O'Neill C (2010) Defects in IGF-1 receptor, insulin receptor and IRS-1/2 in Alzheimer's disease indicate possible resistance to IGF-1 and insulin signalling. *Neurobiol Aging* 31:224–43

Mount PF, Kemp BE, Power DA (2007) Regulation of endothelial and myocardial NO synthesis by multi-site eNOS phosphorylation. *J Mol Cell Cardiol* 42:271–9

Oltman CL, Kane NL, Gutterman DD, Bar RS, Dellsperger KC (2000) Mechanism of coronary vasodilation to insulin and insulin-like growth factor I is dependent on vessel size. *Am J Physiol Endocrinol Metab* 279:E176–81

Oltman CL, Richou LL, Davidson EP, Coppey LJ, Lund DD, Yorek MA (2006) Progression of coronary and mesenteric vascular dysfunction in Zucker obese and Zucker diabetic fatty rats. *Am J Physiol Heart Circ Physiol* 291:H1780–7

Patel MN (2003) Metalloporphyrins improve the survival of Sod2-deficient neurons. *Aging Cell* 2:219–22

Phillips SA, Sylvester FA, Frisbee JC (2005) Oxidant stress and constrictor reactivity impair cerebral artery dilation in obese Zucker rats. *Am J Physiol Regul Integr Comp Physiol* 288:R522–30

Polonsky KS, Given BD, Van Cauter E (1988) Twenty-four-hour profiles and pulsatile patterns of insulin secretion in normal and obese subjects. *J Clin Invest* 81:442–8

Ritchie SA, Kohlhaas CF, Boyd AR, Yalla KC, Walsh K, Connell JM, Salt IP (2010) Insulin-stimulated phosphorylation of endothelial nitric oxide synthase at serine-615 contributes to nitric oxide synthesis. *Biochem J* 426:85–90

Shinozaki K, Nishio Y, Okamura T, Yoshida Y, Maegawa H, Kojima H, Masada M, Toda N, Kikkawa R, Kashiwagi A (2000) Oral administration of tetrahydrobiopterin prevents endothelial dysfunction and vascular oxidative stress in the aortas of insulin-resistant rats. *Circ Res* 87:566–73

Stepp DW (2006) Impact of obesity and insulin resistance on vasomotor tone: nitric oxide and beyond. *Clin Exp Pharmacol Physiol* 33:407–14

Szabo C, Day BJ, Salzman AL (1996) Evaluation of the relative contribution of nitric oxide and peroxynitrite to the suppression of mitochondrial respiration in immunostimulated macrophages using a manganese mesoporphyrin superoxide dismutase mimetic and peroxynitrite scavenger. *FEBS Lett* 381:82–6

Tarpey MM (2002) Sepiapterin treatment in atherosclerosis. *Arterioscler Thromb Vasc Biol* 22:1519–21

Touyz RM (2008) Apocynin, NADPH oxidase, and vascular cells: a complex matter. *Hypertension* 51:172–4

van Veen S, Chang PC (1998) Modulation of vasoconstriction by insulin. *J Hypertens* 16:1157–64

Wang S, Xu J, Song P, Viollet B, Zou MH (2009) *In vivo* activation of AMP-activated protein kinase attenuates diabetes-enhanced degradation of GTP cyclohydrolase I. *Diabetes* 58:1893–901

WHO Expert Committee on Biological Standardization. Thirty-Seventh Report (1987) *World Health Organ Tech Rep Ser* 25–6

Supplementary Information accompanies the paper on the Journal of Cerebral Blood Flow & Metabolism website (http://www.nature.com/jcbfm)